Granular Matter (2020) 22:34
https://doi.org/10.1007/s10035-020-1000-9

ORIGINAL PAPER

Evolution of fabric in spherical granular assemblies under the influence of various loading conditions through DEM

Akhil Vijayan[1] · Yixiang Gan[2] · Ratna Kumar Annabattula[1]

Received: 16 May 2019

Abstract
Fabric of a granular assembly represents the topology of the contact network. This paper investigates the evolution of contact anisotropy (fabric) and average coordination number for a granular assembly subjected to uniaxial compression through the Discrete Element Method (DEM). A monosize three-dimensional random close-packed granular assembly with periodic boundary conditions under uniaxial compression is considered in this work. The fabric evolution is studied by post-processing the output data of the DEM simulation. The influence of cyclic loading, strain rate, and Young's modulus on the evolution of contact anisotropy and average coordination number is presented. The Young's modulus of the particle shows a significant influence on the particle contact creation during compression of the granular assembly with high strain rate. Effect of inertia on the contact anisotropy is observed to be significant during the compression of granular assemblies with different Young's modulus under high strain rate. The paper concludes with a semi-empirical model to predict the evolution of contact anisotropy as a function of the macroscopic stress state of the assembly during quasi-static uniaxial compaction. The model also introduces two microscopic non-dimensional parameters that are independent of friction between the particles and can be used to relate the macroscopic stresses with the contact anisotropy.

Keywords Contact network · Discrete element modelling · Fabric · Contact anisotropy · Coordination number · Granular materials · Packed bed

1 Introduction

Granular systems are ubiquitous in nature from sand piles in deserts to the snow-clad surfaces in the poles. They are an integral part of our everyday life, starting from coffee beans, food grains, construction materials such as cement, gravel, soil, and fertilizers used in agriculture, to name a few. The behavior of the various granular systems described above is highly complex, primarily due to the discrete nature of the constituent particles in addition to the variety of multi-body interactions. The design of various systems employing granular materials requires a thorough knowledge of their response (mechanical, thermal, and electrical) to the external stimulus. The mechanical and thermal response of a granular assembly of particles depends on various parameters such as the bulk mechanical and thermal properties of the particles, the nature of contact interactions between the particles, particle size distribution, and topology of the particle packing.

In a mechanically loaded granular assembly, the forces are transmitted through the contact points between each particle pair. The network depicting the contact normals across the entire granular assembly is called "fabric" or "contact network". The evolution of fabric in a sand pile during external loading was first reported by Oda [1–4]. The contact network represents the force chains when the system is subjected to an external load. The topology of the contact network is responsible for the thermal and mechanical response of a granular assembly subjected to an external load. For example, two-dimensional granular assembly, as shown in Fig. 1a, the polar plot (Fig. 1b) of the number of contacts with respect to their orientation represents the fabric of the granular assembly. The orientation data, i.e., *the number of contacts and their corresponding orientations*, is a measure of the degree of "contact anisotropy" of the system. In the literature, the contact

✉ Ratna Kumar Annabattula
ratna@iitm.ac.in

[1] Mechanics of Materials Laboratory, Department of Mechanical Engineering, Indian Institute of Technology Madras, Chennai 600036, India

[2] School of Civil Engineering, The University of Sydney, Sydney, NSW 2006, Australia

Published online: 26 February 2020

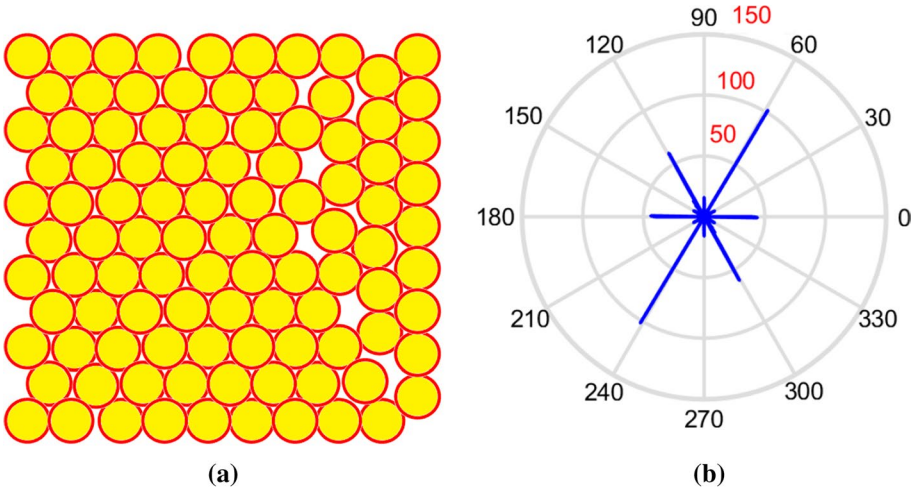

Fig. 1 **a** Two-dimensional mono-size granular assembly. **b** Polar plot of the number of contacts in each direction of the two-dimensional assembly

anisotropy is also referred to as "fabric anisotropy". The fabric tensor, as proposed by Oda [5], describes the probability density function of the orientation data. Satake [6] used the fabric tensor concept for granular materials. Ken-Ichi [7] formulated and used the concept of fabric tensors to describe the distribution of orientation data in a damaged material element. Madadi et al. [8] has studied about the state of fabric tensor in isotropic, static, friction-less, two-dimensional, polydisperse granular materials. O'Sullivan [9] described the basic approaches to quantify the contact anisotropy with an emphasis on the probability density function approach and fabric tensor approach. In the present work, the fabric tensor approach is used to quantify the degree of contact anisotropy in a granular system with the help of orientation data due to its simple form. Shertzer [10] has explained the concept behind the fabric tensor approach and the associated approximations in defining such a tensor. Radjai et al. [11] has analyzed the geometrical states of granular materials through a fabric tensor involving the coordination number and fabric anisotropy along with its Mohr's circle representation. They have formulated a model that gives the range of the fabric states accessible, using the limit values of coordination numbers. Kruyt [12] had studied the evolution of fabric for a dense and loosely packed two-dimensional polydisperse granular system using discrete element simulations. He had studied the influence of three mechanisms; contact reorientation, contact creation, and contact disruption; in the granular system under constant pressure loading. Annabattula et al. [13] have studied the influence of various parameters such as initial packing fraction, radius ratio, and friction on the stress-strain response of binary and polydisperse granular assemblies. Elementary test like oedometric (or uniaxial) compression on granular assemblies gives us a better understanding of the mechanical response of granular materials. Aspects pertaining to the evolution of anisotropy during the uniaxial loading and unloading for a granular assembly has been addressed in Imole et al. [14]. In literature [15–17], studies regarding the evolution of fabric for granular assemblies under shear loading have also been reported.

Mathematically, the fabric tensor $\boldsymbol{F}$, discussed above is defined as [12]

$$F_{ij} = \frac{1}{N_c} \sum_{c=1}^{N_c} n_i^c n_j^c, \tag{1}$$

where N_c is the number of non-repeating contacts in the assembly, n_i is the normal vector component in ith direction at contact 'c'. Thornton [18] used the difference between the eigenvalues of fabric tensor as a measure of *degree of contact anisotropy* for a 2D granular assembly. It can be extended to 3D case (similar to [11]) where the difference is taken between maximum and minimum eigenvalues. Hence, the *degree of contact anisotropy* (A) is defined as

$$A = F_3 - F_1, \tag{2}$$

where $F_1 < F_2 < F_3$ are the eigenvalues of the fabric tensor $\boldsymbol{F}$. The *average coordination number* (Z) can be written in terms of the number of contacts (N_c) and the total number of particles in the assembly (N_p) as

$$Z = \frac{2N_c}{N_p}. \tag{3}$$

The average coordination number as defined above includes rattlers (particles with only one contact) and floaters (particles with no contact) [14, 18].

Most of the works presented in the literature address either the evolution of fabric [19, 20] in a random granular assembly or the correlation [21–23] of the fabric and its macroscopic response to explain the constitutive behavior under various loading conditions. However, the effect of the compression loading rate [24, 25] on the fabric evolution has been discussed very little in the literature to the best of author's knowledge. Furthermore, the mechanisms behind

the evolution of fabric under cyclic compression loading of a granular assembly have not been investigated thoroughly in the literature. The variation of contact anisotropy during the cyclic loading has the potential to alter the macroscopic properties, such as effective thermal/electrical conductivity. Several prediction models [26–29] correlating the macroscopic stress tensor and the fabric have been proposed in the literature. All the models presented in the literature provide a detailed formulation involving several parameters.

In view of the above research gaps in the literature, the manuscript focuses on the following three objectives:

1. To demonstrate the effect of cyclic loading on the contact anisotropy for a monosize random granular assembly,
2. To consider the effect of loading rate on the contact anisotropy, and
3. To develop a semi-empirical model to correlate fabric tensor and stress tensor with a minimal number of parameters.

The evolution of fabric in a periodic granular assembly under uniaxial compression is studied in Sect. 2. The results of the simulations for the first loading cycle of the periodic assembly are presented in Sect. 2.3.1. In Sect. 2.3.2, the evolution of contact anisotropy during cyclic loading of the granular assembly has been discussed. The influence of strain rate (or loading rate) of compression and Young's modulus of the particle on the evolution of contact anisotropy is discussed in Sects. 3 and 4, respectively. In Sect. 5, a semi-empirical model to establish a correlation between the stress tensor and fabric tensor is discussed. The paper completes with conclusions in Sect. 6.

2 Evolution of contact anisotropy in a periodic granular assembly under uniaxial compaction

In this section, the evolution of contact anisotropy for a random granular assembly with periodic boundary conditions under uniaxial[1] cyclic compression is presented. First, the details of the methodology of the generation of the initial configuration of particles are presented. It is then followed by the description of the DEM simulation set-up and the corresponding boundary conditions.

[1] Strictly speaking, the state of stress in the granular assembly with the present kind of loading is not uniaxial. However, in this work, we use *uniaxial*, referring to the loading which is applied only in one direction.

2.1 Generation of initial configurations of granular assemblies

The initial configuration of the granular assembly is generated using the Random Close Packing algorithm proposed by Jodrey and Tory [30] for mono-sized spheres. The required number of spherical particles are generated in a cube. Initially, the particles are overlapped and their respective radii are set in such a way that the packing fraction is 1. During each iteration of the procedure, two numerical mechanisms are concurrently followed in-order to arrive at the final configuration. One, the worst overlaps are removed by moving two particles away along the contact normal of the particles. Two, the radii of particles are reduced incrementally for relaxation. Hence, the final configuration of the assembly will have a very less number of particles in contact while most of the particles are nearly touching each other. This structure resembles the state of the bulk region in a granular bed confined by the container boundaries. The final configuration can be scaled to any size as per the required particle size. It may be noted that the initial packing structure, obtained through this algorithm, is necessarily not in a jammed state. Every configuration used in the present work is characterized by the *initial packing fraction* (η), which is only the starting configuration of the simulation. During compression, the particles in the assembly rearrange and move from an unjammed state to a jammed state where the particle movements become negligible. Also, since the granular assembly is under uniaxial compression, the instantaneous packing fraction of the assembly is proportional to the instantaneous strain. Hence, strain is chosen as the independent variable throughout the work.

2.2 Details of the simulation setup

Discrete element method (DEM) [31] is used to simulate the compression of a random granular assembly. DEM simulations are carried out using the open source DEM software LIGGGHTS [32]. A granular assembly of 5000 monodisperse particles in a periodic cubic box as shown in Fig. 2 is taken as a representative volume element (RVE). The granular assembly is uniaxially compressed to a macroscopic strain of 1.5% unless mentioned otherwise. In the simulations, the effect of gravity is not considered. The particles are assumed to be spherical with a Poisson's ratio (ν) of 0.25 and an elastic modulus (E) of 90 GPa. The normal contact interaction between the particles is assumed to be elastic following Hertzian contact model. The tangential contact force is based on the tangential overlap and tangential relative velocity. The inter-particle contact force ($\mathbf{f}_{ij}$) between particles i and j can be written as [33],

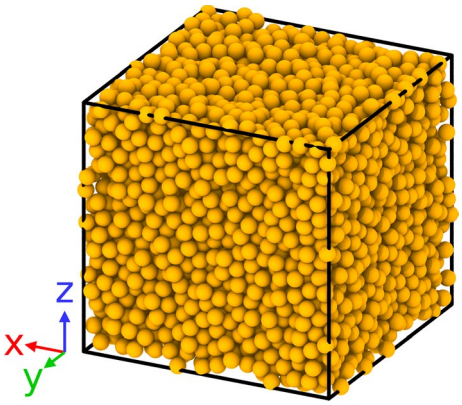

Fig. 2 RVE of a mono-size granular assembly with periodic boundaries

$$\mathbf{f}_{ij} = \underbrace{(k_n \boldsymbol{\delta}_{ij}^n - \gamma_n \mathbf{v}_{ij}^n)}_{\text{Normal force}} + \underbrace{(k_t \boldsymbol{\delta}_{ij}^t - \gamma_t \mathbf{v}_{ij}^t)}_{\text{Tangential force}}, \tag{4}$$

where,

$$k_n = \frac{4}{3} E^* \sqrt{R^* \delta^n}; \; k_t = 8 G^* \sqrt{R^* \delta^n}, \tag{5}$$

$$\begin{aligned} \gamma_n &= 2\sqrt{\frac{5}{6}} \beta \sqrt{2 E^* \sqrt{R^* \delta^n m^*}}; \\ \gamma_t &= 2\sqrt{\frac{5}{6}} \beta \sqrt{8 G^* \sqrt{R^* \delta^n m^*}} \; (\gamma_n, \gamma_t \geq 0), \end{aligned} \tag{6}$$

$$\beta = \frac{\ln(e)}{\sqrt{\ln^2(e) + \pi^2}}; \; \frac{1}{E^*} = \frac{1 - \nu_i^2}{E_i} + \frac{1 - \nu_j^2}{E_j}, \tag{7}$$

$$\frac{1}{G^*} = \frac{2(2 - \nu_1)(1 + \nu_1)}{E_i} + \frac{2(2 - \nu_2)(1 + \nu_2)}{E_j}, \tag{8}$$

$$\frac{1}{R^*} = \frac{1}{R_i} + \frac{1}{R_j}; \; \frac{1}{m^*} = \frac{1}{m_i} + \frac{1}{m_j}. \tag{9}$$

In the above equations, ν, E, G, e, R and m represents Poisson's ratio, Young's modulus, shear modulus, coefficient of restitution, particle radius and the mass of the particles i and j in contact, respectively. The terms $\boldsymbol{\delta}_{ij}^n$, $\boldsymbol{\delta}_{ij}^t$, $\mathbf{v}_{ij}^n$ and $\mathbf{v}_{ij}^t$ represents the normal overlap, tangential overlap, normal relative velocity and tangential relative velocity, respectively, between particles i and j in contact. The tangential overlap is truncated by limiting the maximum tangential force which can be stated by Coulomb's law of friction as $\mathbf{f}_t \leq \mu \mathbf{f}_n$. Hence, the tangential force can be expressed as,

$$\mathbf{f}_t = -\frac{\mathbf{v}_{ij}^t}{|\mathbf{v}_{ij}^t|} min\Big(\mu \mathbf{f}_n, k_s |\mathbf{v}_{ij}^t| . \Delta t\Big), \tag{10}$$

where, $\mathbf{f}_t$, μ, and $\mathbf{f}_n$ are the tangential force, coefficient of friction and the normal contact force, respectively while k_s represents the coefficient (in the case of small tangential displacement) which is proportional to the sliding velocity. The coefficient of friction between the particles is assumed to be 0.1 if not mentioned otherwise. The possibility of particle breakage during loading is not considered in this work.

2.3 Results and discussion

The granular assembly shown in Fig. 2 is compressed uniaxially resulting in the particles movement and rearrangement leading to evolution of contact force network. With increase in compression, the particles come closer and hence approach a saturated or jammed state where no further rearrangement is possible. During the above process, the evolution of contact anisotropy depends on the boundary conditions and the nature of loading significantly. In the following section, we discuss the effect of uniaxial compression on the evolution of contact anisotropy and average coordination number. It is then followed by a study of the evolution of contact anisotropy during cyclic loading of the system for 5 consecutive cycles.

2.3.1 Periodic granular assembly under uniaxial compression

Figure 3 shows the evolution of fabric characteristics during the compression of a monosize granular assembly in negative Z direction. It can be inferred from Fig. 3a that the contact anisotropy of the granular assembly increases with increase in strain. Eigenvalues (Fig. 3b) of the fabric tensor are an equivalent representation of the contribution of the components of all the contact normals in the principal directions. Hence, studying the evolution of eigenvalues will provide a better insight to the mechanism behind the particle rearrangement taking place in the granular assembly. From Fig. 3b, it can be inferred that the rate of increase of the number of contacts in the assembly is higher in one direction (aligned closely to Z-axis i.e. direction of loading) as compared to other directions (aligned closely to transverse axes), thus leading to increase in the anisotropy of the assembly. Also note that the average coordination number of the assembly increases (result not shown) with increase in strain. However, the average coordination number saturates beyond a certain strain value corresponding to the jammed state of the assembly implying a sharp drop in the intensity of particle rearrangement. A tightly packed system will attain saturated state faster than a loosely packed system due to the limited mobility of particles.

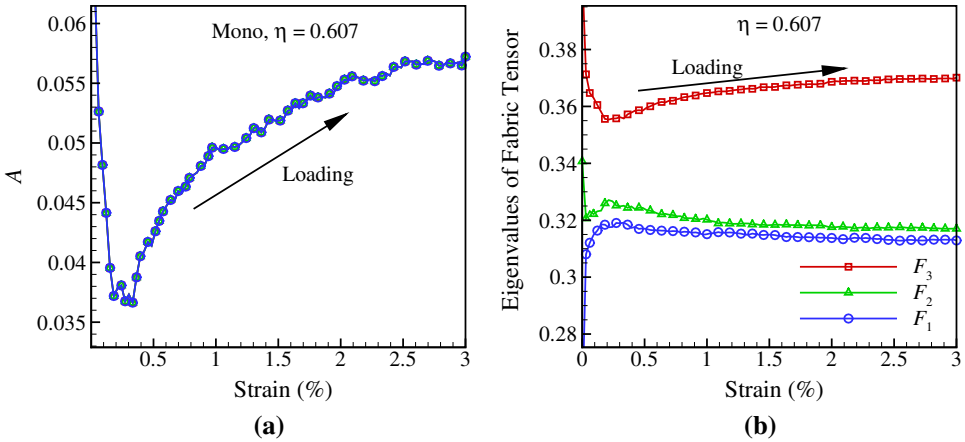

Fig. 3 **a** Evolution of contact anisotropy A and **b** eigenvalues of the fabric tensor during uniaxial compression of a mono-size granular assembly with initial packing fraction (η) of 0.607

2.3.2 Effect of cyclic loading on the fabric characteristics

In this section, the evolution of contact anisotropy under the action of cyclic loading/unloading is studied. The granular assembly is loaded to 1.5% strain followed by unloading to a stress free state for 5 cycles. Figure 4a shows the evolution of contact anisotropy as a function of strain for five consecutive loading-unloading cycles. The solid lines indicate the loading step while the dashed lines indicate the unloading step. There is a point of minimum contact anisotropy, referred to as a *critical point* in the following. In the first cycle of loading, the contact anisotropy increases continuously while during unloading to stress free state, the contact anisotropy decreases to a minimum value and then increases with steep slope. In other words, the anisotropy of the assembly is a multi-valued function of strain, i.e., the system shows the same anisotropy value at two different strains during a given loading or unloading cycle. Each component of the fabric tensor indicates the contribution of all contact normals along that axis plus the projection of the remaining contact normals on to the axis. From Fig. 4b, it can be observed that the effective number of contact normals along Z axis (Z-directional contacts) decreases to a very low value as compared to X (and Y) directional contacts for each unloading cycle. The point where the three diagonal components of fabric tensor becomes almost equal represents the critical point mentioned above. Thus, the critical point indicates a state where the effective number of contact normals in all the three coordinate directions are the same. It also implies that an assembly, if pre-loaded appropriately, can attain a configuration with minimum anisotropy. Granular assemblies with minimum possible anisotropy could be of interest to obtain, for instance, systems with near-isotropic thermal conduction or force networks. However, with further unloading beyond the critical point, the difference between F_{ZZ} and F_{XX} increases due to steep drop in F_{ZZ}. As a result, we observe an increase in anisotropy beyond the critical point during unloading as shown in Fig. 4a. Furthermore, after each loading-unloading cycle, the effective number of lateral (X and Y) contacts increases more than the contacts in the loading direction (Z). Hence, we can observe a slight decrease in contact anisotropy with each cycle of loading (also observed for the load/unload triaxial tests by O'Sullivan and Cui [34]). This indicates that the uniaxial

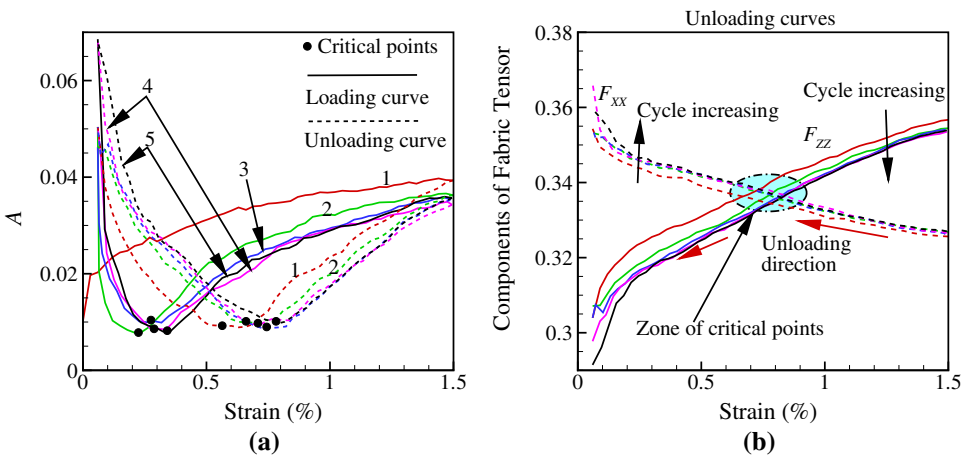

Fig. 4 Evolution of **a** contact anisotropy during loading and unloading cycles. **b** components of fabric tensor (F_{XX} and F_{ZZ}) during unloading. The numbers near the lines in the plot represent the cycle number

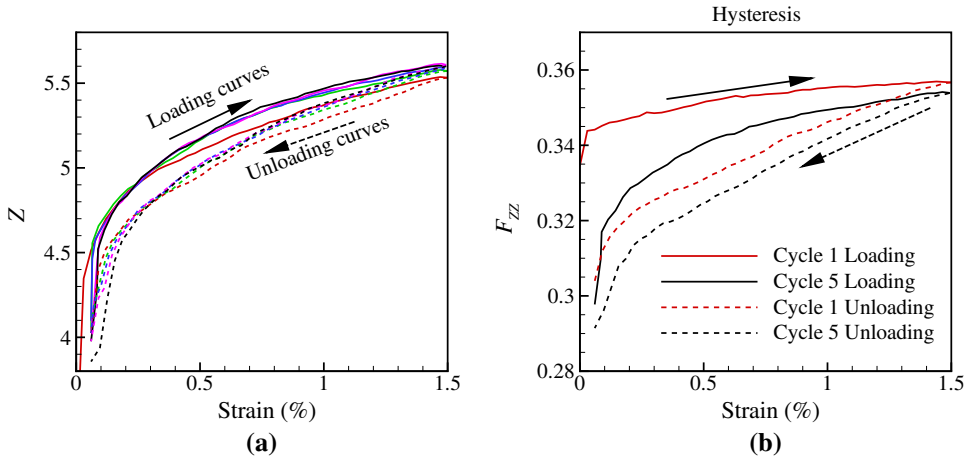

Fig. 5 **a** Evolution of average coordination number during loading and unloading cycles. **b** Evolution of F_{ZZ} during loading-unloading cycles 1 and 5

cyclic loading and unloading will lead to less anisotropic configurations of the granular assembly on contrary to the case of granular assemblies under cyclic constant volume loading (Soroush and Ferdowsi [35]).

From Fig. 5a, it can be observed that there is a hysteresis in the states of evolution of average coordination number during loading and unloading cycles. Such a behavior is also observed in the stress-strain response of the granular assemblies [13]. The hysteretic stress-strain response may be attributed to the hysteretic behavior of the Z-directional contacts as shown in Fig. 5b. Similar hysteretic behavior (inverted curve) is also present in the case of X and Y directional contacts (results not shown). Thus, the hysteresis curve of Z-directional contacts can be directly correlated with stress-strain hysteresis curve due to similar nature. Hence, the fabric characteristics of contacts can be used directly in the constitutive modelling (also shown for shearing of granular assembly by Sun and Sundaresan [36]) of granular assemblies during compression.

3 Influence of strain rate on the evolution of contact anisotropy during compression of a periodic granular assembly

Note that the results presented in the previous sections (Sects. 2.3.1–2.3.2) correspond to the quasi-static compression of the granular assembly. In this section, the effect of strain rate on the evolution of anisotropy is studied during the compression of a periodic granular assembly. All the system parameters used in the simulations remain the same as described in Sect. 2.2. A monosize particle assembly (5000 particles) with periodic boundary conditions is loaded till 3% strain at different strain rates ($\dot{\epsilon}$ = 1500/s, 150/s,15/s,0.15/s). A granular system can be classified to be in a quasi-static regime or in a dense flow regime or in a collisional dilute flow regime based on the inertial number (I) of the system. The inertial number is defined as the ratio of the inertial forces on the grains to the applied force. The inertial number[2] for the granular assemblies loaded at different strain rates as mentioned above is calculated following MiDi [37], where the shear strain rate is replaced by the compression strain rate ($\dot{\epsilon}$) as shown in Eq. 11

$$I = \frac{\dot{\epsilon}\, d}{\sqrt{P/\rho}}, \tag{11}$$

where d is the particle diameter, P is the compressive stress and ρ is the density of the material. Based on the value of I, the granular flow regimes are characterized according to

$I < 10^{-3}$	quasi-static flow regime,
$10^{-3} < I < 10^{-1}$	dense flow regime,
$I > 10^{-1}$	collisional dilute regime.

Figure 6 shows the periodic granular assembly with the colors representing the coordination number when loaded at $\dot{\epsilon}$ =1500/s at three different stages during loading. Based on the value of inertial number ($I = 1.253 \times 10^{-2}$), the assembly is under dense flow regime. It may be noted that at such a high strain rate, the coordination number for the particles near the boundaries is highest and minimum at the center at a given strain. However, with the increase in strain in the assembly, the coordination number increases towards the central region of the assembly. Figure 7 shows the granular assemblies at different loading stages depicting their coordination numbers when loaded at a very low strain rate corresponding to quasi-static case with $I = 1.324 \times 10^{-6}$. Figure 8 shows the evolution of A and Z as a function of strain for different strain rates. Note that the inertial numbers corresponding to each strain rate fall

[2] I is calculated by taking the maximum value of pressure developed in the system.

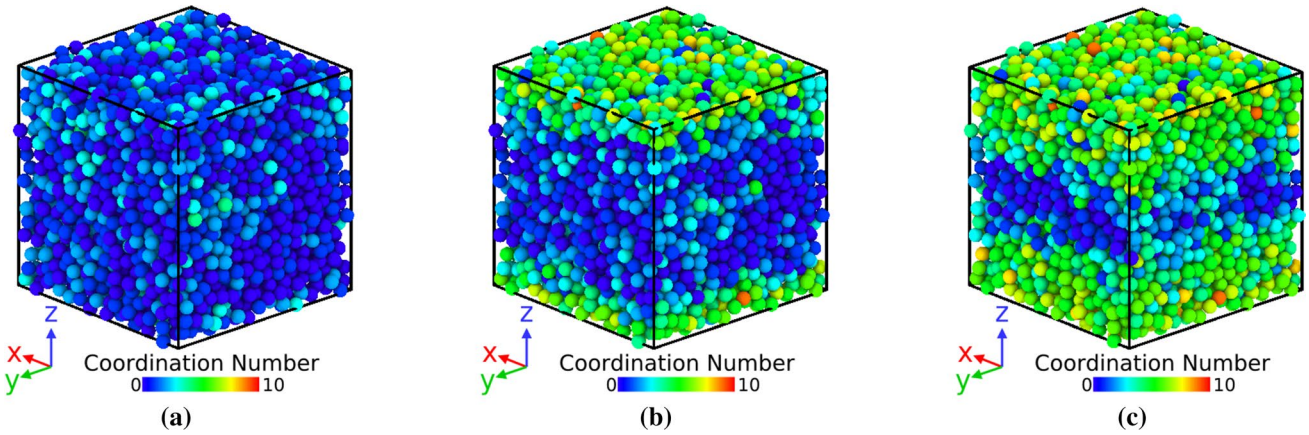

Fig. 6 Instantaneous coordination number distribution during compression ($\dot{\epsilon}$ =1500/s, $I = 1.253 \times 10^{-2}$) at a macroscopic strain (**a**) $\epsilon_{33} = 0\%$ (**b**) $\epsilon_{33} = 0.375\%$ and (**c**) $\epsilon_{33} = 0.75\%$

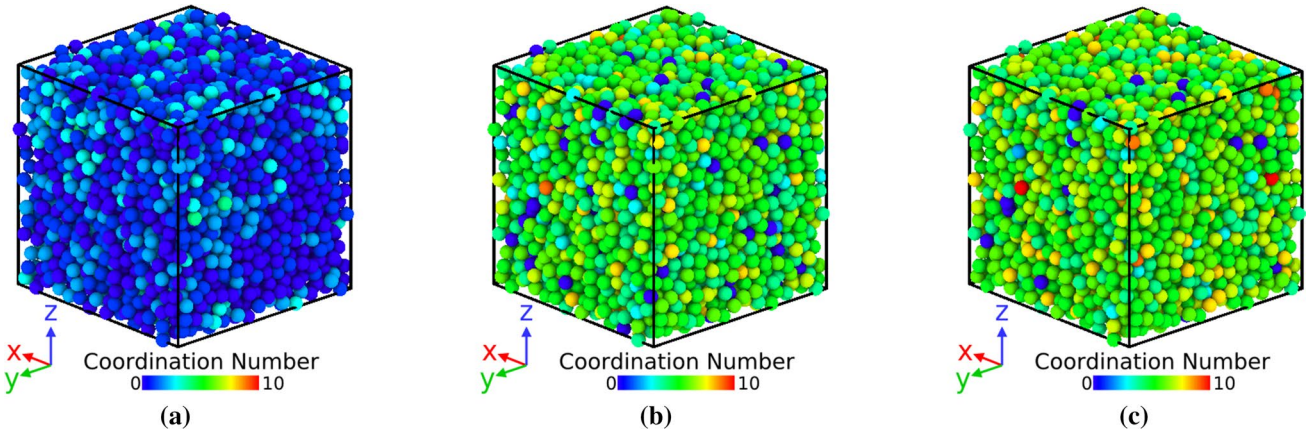

Fig. 7 Instantaneous coordination number distribution during compression ($\dot{\epsilon} = 0.15$/s, $I = 1.324 \times 10^{-6}$) at a macroscopic strain (**a**) $\epsilon_{33} = 0\%$ (**b**) $\epsilon_{33} = 0.375\%$ and (**c**) $\epsilon_{33} = 0.75\%$

between quasi-static and dense flow regimes. In the case of quasi-static compression (Fig. 7) with $\dot{\epsilon} = 0.15$/s , the contact between particles evolve uniformly over the whole assembly at each loading stage. Hence, there is higher average coordination number (see Fig. 8b) for low strain rates as compared to high strain rate during the initial stage. In the case of high strain rate ($\dot{\epsilon} = 1500$/s), the top and bottom layers will have more contacts in Z-direction as compared to X and Y (results not shown). Hence, the steep increase of Z-directional contacts will increase the anisotropy drastically at initial stage (Fig. 8a) which drops eventually due to increase of contacts in transverse directions with increase in strain. Note that the coordination number and the contact anisotropy values approach the same value at higher strains irrespective of the strain rate of loading. This zone is a high stress zone, possibly in a jammed state, which will most likely lead to particle breakage. Thus, the effect of strain rate on the evolution of fabric characteristics can be considered only as a transient phenomenon.

4 Influence of Young's modulus on the evolution of contact anisotropy during compression of a periodic granular assembly

In this section, the influence of the particle elastic modulus on the evolution of contact anisotropy during compression is studied. A monosize granular assembly of 5000 particles (Periodic Boundary Conditions as in Sect. 2.2) with different elastic modulus is loaded till 3% strain quasi-statically and with high strain rate.

Figure 9 shows the evolution of contact anisotropy and the coordination number as a function of strain for assemblies

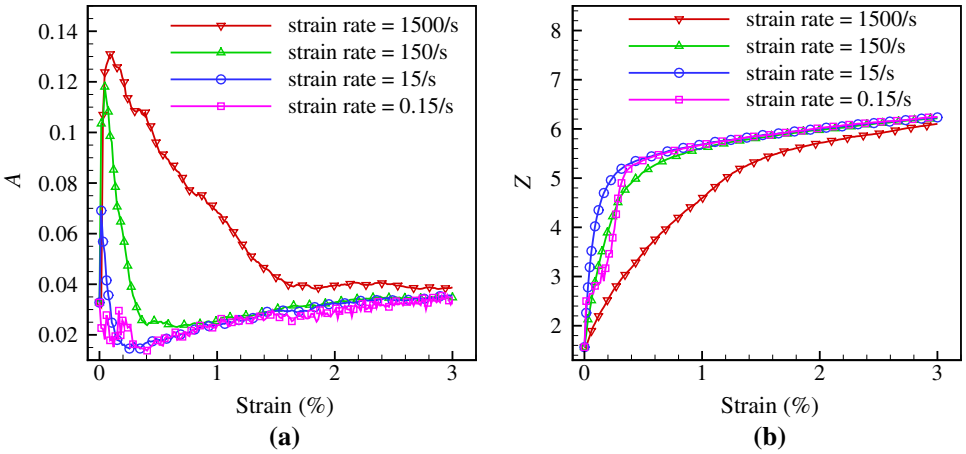

Fig. 8 Evolution of **a** contact anisotropy (A) and **b** average coordination number (Z) for a mono-size granular assembly with different strain rates. Inertial numbers of the system are 1.325×10^{-6} ($\dot{\epsilon} = 0.15$/s), 1.287×10^{-4} ($\dot{\epsilon} = 15$/s), 1.281×10^{-3} ($\dot{\epsilon} = 150$/s) and 1.253×10^{-2} ($\dot{\epsilon} = 1500$/s)

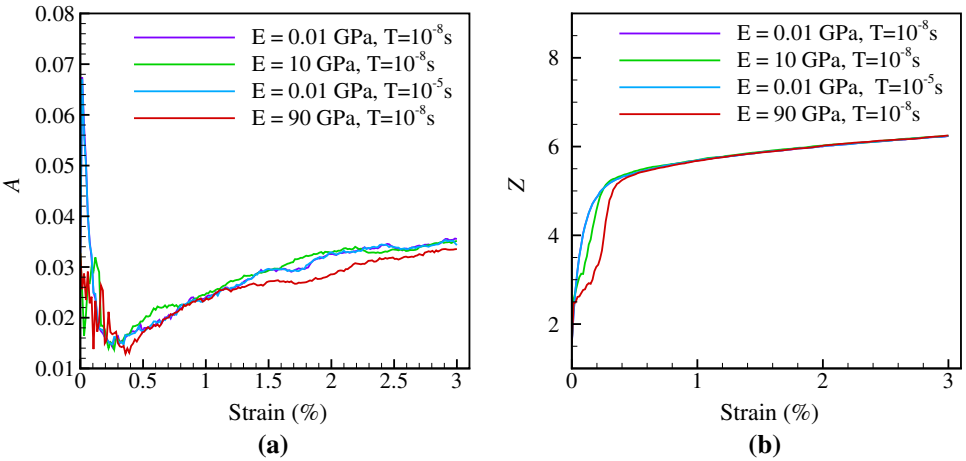

Fig. 9 Evolution of **a** contact anisotropy (A) and **b** average coordination number (Z) for a mono-size granular assembly with different elastic modulus during quasi-static compression

with different elastic modulus. It can be observed that there are no significant changes in the evolution of anisotropy and the coordination number during quasi-static compression. It is also worth noticing how the case of E= 90 GPa, time step $T = 10^{-8}$s matches closely with the case of E= 0.01 GPa, $T = 10^{-5}$s. Note that all the above simulations with different values of E were conducted at a strain rate $\dot{\epsilon}$=15/s and the inertia number[3] for the four different E values correspond to quasi-static loading ($I \leq 10^{-3}$). Hence, the inertia doesn't seem to influence the anisotropy evolution for different values of E.

During compression of soft particles with high strain rate, the average particle interpenetration will be high as compared to that of hard particles. Also, for soft particles, due to reduced elastic modulus the inter-particle forces generated will be very less. Due to lesser forces between soft particles, the process of contact creation between particles will be slow as compared to hard particles as shown in Fig. 10. Such contact creations give rise to higher anisotropy as seen in Fig. 11. Note that in Fig. 11, the anisotropy for the systems with $E \geq 5$ GPa is observed to be independent of the elastic modulus as the inertial number for $E \geq 5$ GPa is close to quasi-static regime ($I \leq 6 \times 10^{-3}$). For the case of $E = 5$ and 50 MPa, the inertial numbers are close to collisional dilute regime ($I \geq 0.09$) explaining the dependence of the anisotropy on the elastic modulus.

5 Semi-empirical prediction of contact anisotropy based on macroscopic stresses

In this section, a semi-empirical correlation connecting the fabric tensor and the macroscopic stress of a granular assembly will be presented.

5.1 Simplified form of the stress tensor

The tensor form of average macroscopic stress of a granular assembly is given by

[3] The inertial number I is calculated by replacing P with E in Eq. 11.

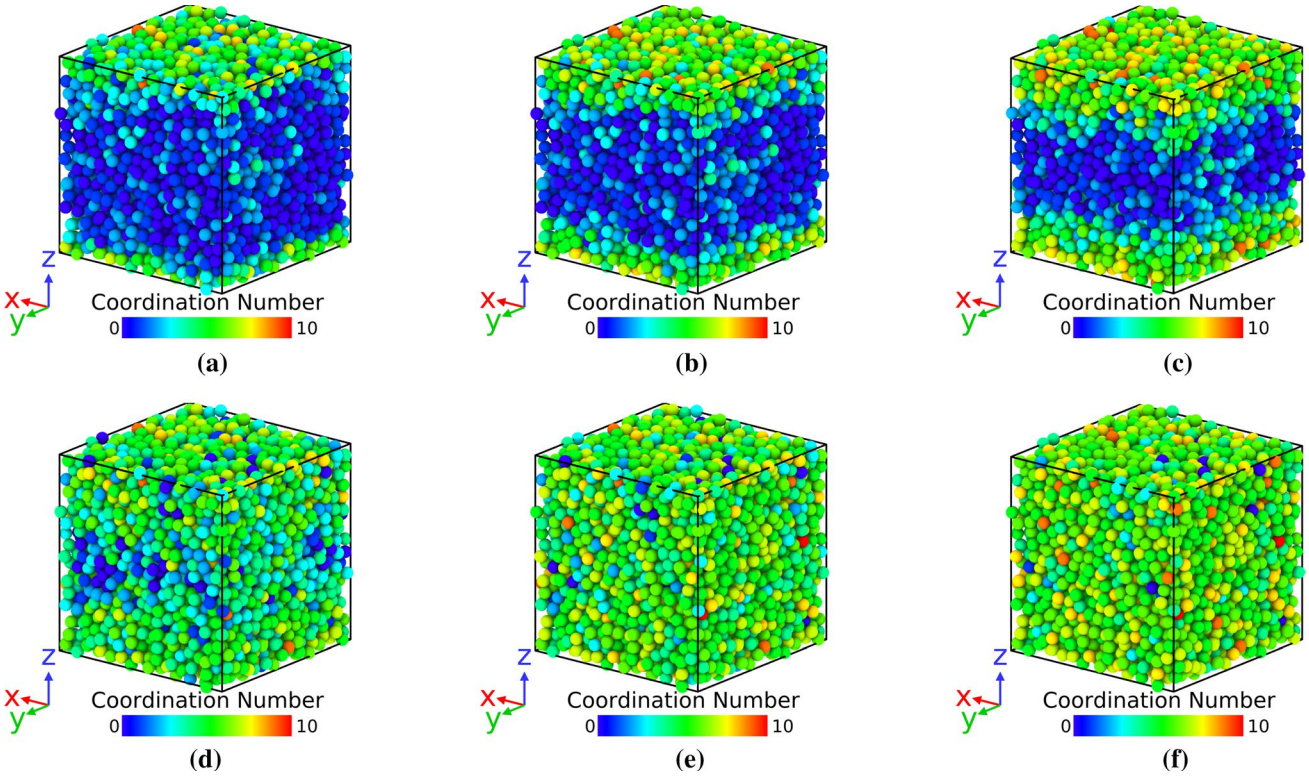

Fig. 10 Instantaneous coordination number distribution during compression with high strain rate ($\dot{\epsilon}$ = 150/s) of particles with elastic modulus 50 MPa (**a**, **b**, **c**) and 50 GPa (**d**, **e**, **f**) at strain of 0.3% (**a**, **d**), 0.75% (**b**, **e**) and 1.5% (**c**, **f**)

Fig. 11 Evolution of **a** contact anisotropy (A) and **b** average interpenetration (δ) between particle pairs for a mono-size granular assembly with different elastic modulus during compression with high strain rate

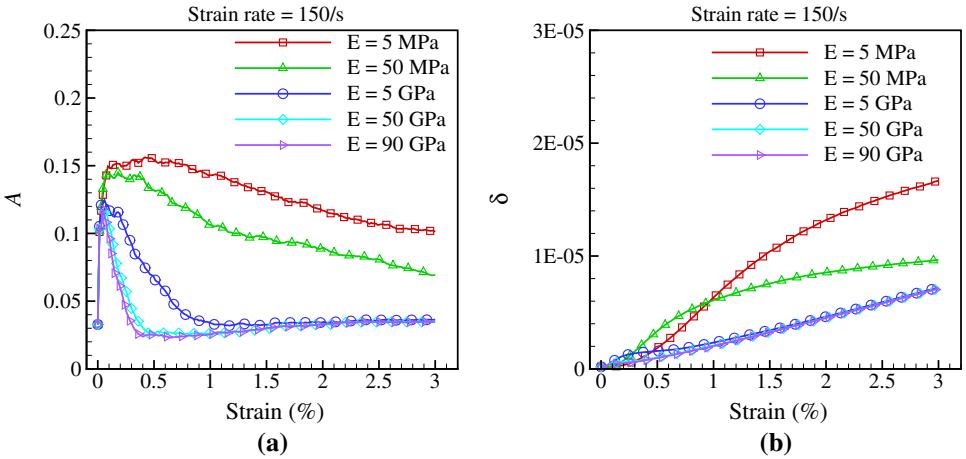

$$\overline{\sigma}_{ij} = \frac{1}{V}\sum_{I<J}\left(\delta^{(I,J)}\mathbf{f}_n^{(I,J)}n_i n_j + \delta^{(I,J)}\mathbf{f}_t^{(I,J)}n_i t_j\right), \tag{12}$$

where $\delta^{(I,J)}$ is the inter-particle center distance, n_i and t_i are the component of unit normal contact vector and unit tangential vector in the ith direction between the contacting particles as shown in Fig. 12.

During the uniaxial compression of granular assemblies, contribution of tangential forces ($\mathbf{f}_t$) is negligible compared to normal forces ($\mathbf{f}_n$). Figure 13 shows the relative deviation of stress values caused by neglecting the tangential force terms to be always less than ±6% for the systems under consideration. Hence, neglecting the second term in Eq. 12, we can rewrite,[4]

[4] The assumption of neglecting the tangential term is to simplify the stress tensor calculation only.

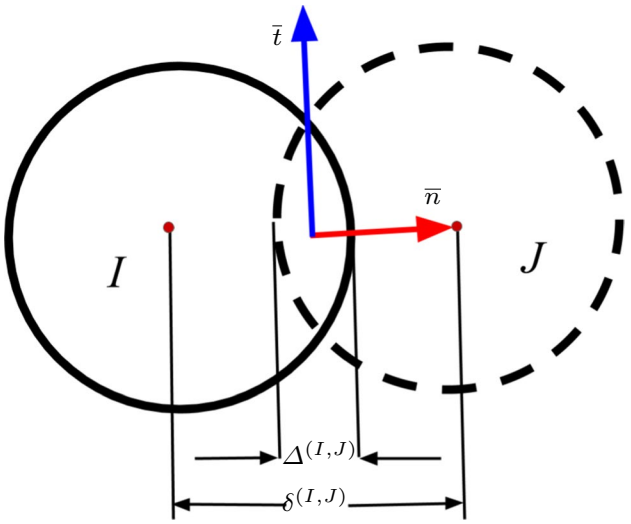

Fig. 12 A two-dimensional idealization of inter-particle interaction between particles 'I' and 'J'. $\bar{n}$ and $\bar{t}$ represents the direction of normal force and tangential force

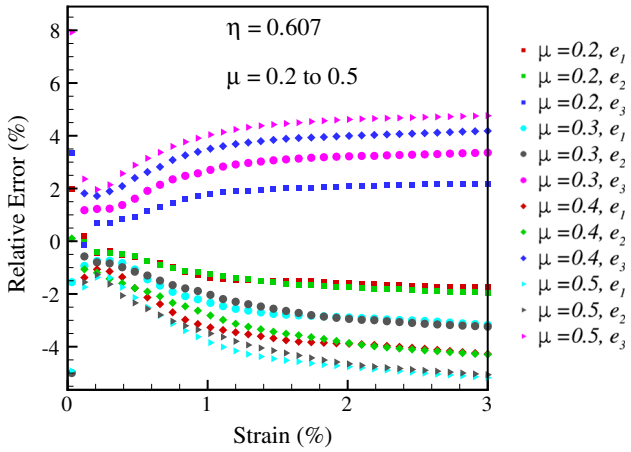

Fig. 13 Relative error in macroscopic stress caused by neglecting the tangential force term for an assembly with initial packing fraction $\eta = 0.607$ and $0.2 \leq \mu \leq 0.5$. In the colour map, the variable e_i (i = 1, 2 and 3) represents the relative error for σ_{ii} component of stress tensor. The relative error is less than ± 6% (results not shown) for the assemblies with different initial packing fractions in the range $0.594 \leq \eta \leq 0.64$ for a range of friction coefficients ($0.1 \leq \mu \leq 0.9$)

$$\overline{\sigma}_{ij} = \frac{1}{V} \sum_{I<J} \delta^{(I,J)} \mathbf{f}_n^{(I,J)} n_i n_j. \tag{13}$$

For mono-size particle assembly, the separation variable $\delta^{(I,J)} = d_p - \Delta^{(I,J)}$ where $\Delta^{(I,J)}$ is the contact overlap between the particles I and J while d_p is the diameter of the particle. Since the normal force is a function of the inter-penetration [38] between the particles, it is reasonable to neglect the terms of $O(\Delta^2)$ for small overlapping contacts. Hence, the macroscopic stress $\overline{\sigma}_{ij}$ can be further simplified to

$$\overline{\sigma}_{ij} = \frac{d_p}{V} \sum_{I<J} \mathbf{f}_n^{(I,J)} n_i n_j. \tag{14}$$

Equation 14 can be written in terms of instantaneous packing fraction (η_f), average coordination number (Z) and number of contacts (N_c) as,

$$\overline{\sigma}_{ij} = \frac{3\eta_f Z}{\pi d_p^2 N_c} \sum_{1}^{N_c} \mathbf{f}_n^{(I,J)} n_i n_j \tag{15}$$

Normal force term ($\mathbf{f}_n$) can be expressed in terms of contact radius 'a' [39] which can be rewritten as

$$\overline{\sigma}_{ij} = \frac{\beta}{N_c} \sum_{1}^{N_c} a^3 n_i n_j, \tag{16}$$

where $\beta = \frac{4\eta_f Z}{\pi d_p^2} \frac{E^*}{R^*}$. Note that, η_f and Z are the instantaneous packing fraction and the average coordination number, respectively while E^* and R^* represent the effective Young's modulus and the reduced radius for a contact pair.

5.2 Redefining the contact anisotropy

Alternative measure of contact anisotropy was presented by [40] which is the ratio of the maximum and minimum eigenvalues instead of its difference. Hence, another form of contact anisotropy can be written as

$$A_r = \frac{F_3}{F_1} \tag{17}$$

Figure 14 suggests that both the measures works well to qualitatively capture the evolution of contact anisotropy. Hence, the new measure of anisotropy A_r is chosen over A for further investigations in this manuscript. It may be noted that the new definition is chosen only for simplification purpose.

5.3 Assumptions

In addition to the above considerations, a few assumptions for the case of uniaxial compression of the granular assembly are in order as described below. These assumptions will be used in later sections to simplify equations.

– **Assumption 1**
  During uniaxial compression of any granular assembly in negative Z-direction (i.e. along 3rd direction), the values of transverse directional stresses i.e. σ_{11} and σ_{22} are close to each other. The closeness will depend on the contact orientation along transverse directions. If we assume that the orientation of particle pair contact vectors along both transverse direction is same (for example,

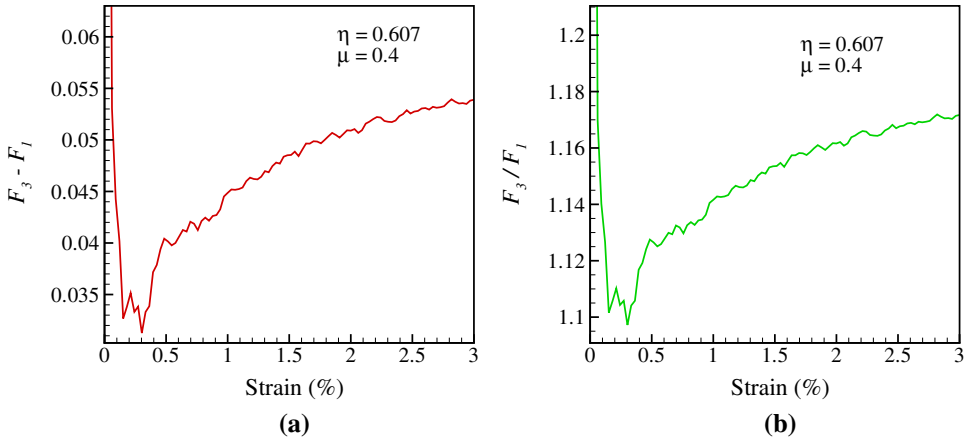

Fig. 14 Comparison of measures of contact anisotropy (**a**) A (**b**) A_r for an assembly with η of 0.607

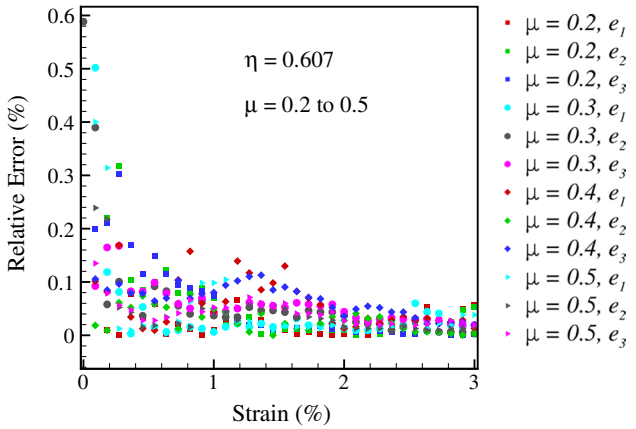

Fig. 15 Percentage deviation of diagonal components of fabric tensor from its eigenvalues for an assembly with η of 0.607 and μ ranging from 0.2 to 0.5. In the colour map, the variable e_i (i = 1, 2 and 3) represents the relative error between the component F_{ii} and the corresponding eigenvalue F_i

see the closeness of eigenvalues in Fig. 3b), then it can be assumed that

$$F_{11} = F_{22} \tag{18}$$

$$\text{also, } F_{11} + F_{22} + F_{33} = 1 \tag{19}$$

– **Assumption 2**

During uniaxial compression of any granular assembly, the contact chains align along the loading direction. Due to this the value of diagonal components of fabric tensor (F_{33}, F_{22} and F_{11}) are very close to the eigen values of the fabric tensor. Fig. 15 shows the relative error or deviation of the diagonal components of fabric tensor from its eigenvalues for an assembly with η of 0.607 and μ ranging from 0.2 to 0.5. The result is verified for assemblies with different initial packing fraction in the range $0.607 \leq \eta \leq 0.64$. Therefore, the anisotropy of the granular assembly can be approximated using the diagonal terms of the fabric tensor also. Hence, the anisotropy can be rewritten as,

$$A_r = \frac{F_3}{F_1} = \frac{F_{33}}{F_{11}} \text{ (assuming } F_{11} \text{ is minimum)} \tag{20}$$

5.4 Correlating stress ratio and fabric ratio

Assume two non-dimensional variables stress ratio (σ_r) and fabric ratio (ϕ_r) which are defined as below.

$$\sigma_r = \frac{\sigma_{33}}{\sigma_{11} + \sigma_{22}} = \frac{\sum a^3 n_3^2}{\sum a^3 n_1^2 + \sum a^3 n_2^2} \text{ (from Eq. 16)} \tag{21}$$

$$= \frac{\sum a^3 n_3^2}{\sum a^3 - \sum a^3 n_3^2} = \frac{1}{\frac{\sum a^3}{\sum a^3 n_3^2} - 1} \tag{22}$$

$$\phi_r = \frac{F_{33}}{F_{11} + F_{22}} = \frac{\frac{\sum n_3^2}{N_c}}{\frac{\sum n_1^2 + \sum n_2^2}{N_c}} = \frac{\sum n_3^2}{\sum n_1^2 + \sum n_2^2} = \frac{\sum n_3^2}{\sum 1 - \sum n_3^2} \tag{23}$$

$$= \frac{1}{\frac{\sum 1}{\sum n_3^2} - 1} = \frac{1}{\frac{1}{F_{33}} - 1} \tag{24}$$

Here, the symbol $\sum$ indicates the summation of the quantity over the total number of contacts between particles in the assembly. Assume two non-dimensional quantities R_σ and R_ϕ where $R_\sigma = \frac{\sum a^3}{\sum a^3 n_3^2}$ and $R_\phi = \frac{1}{F_{33}}$. Figure 16 shows the evolution of the non-dimensional quantities for different values of

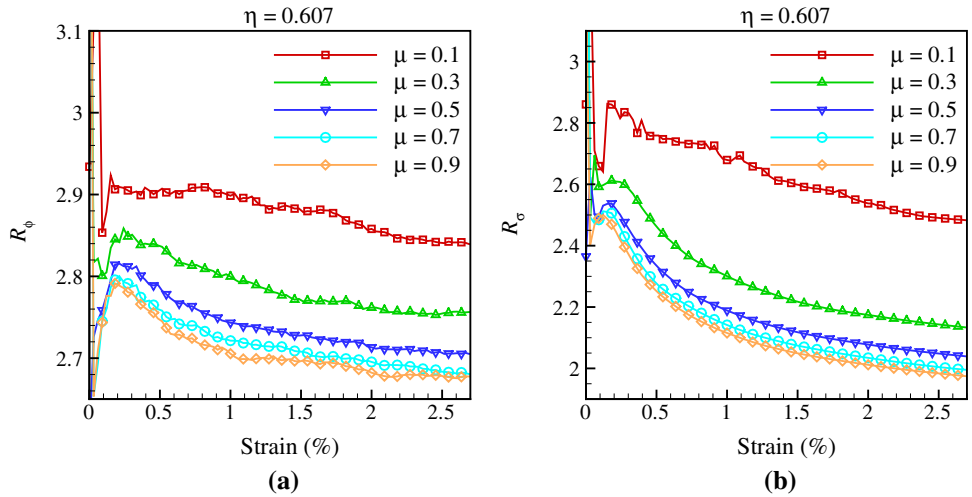

Fig. 16 Evolution of parameters (**a**) R_ϕ and (**b**) R_σ with different coefficient of friction during the uniaxial compression of periodic granular assemblies

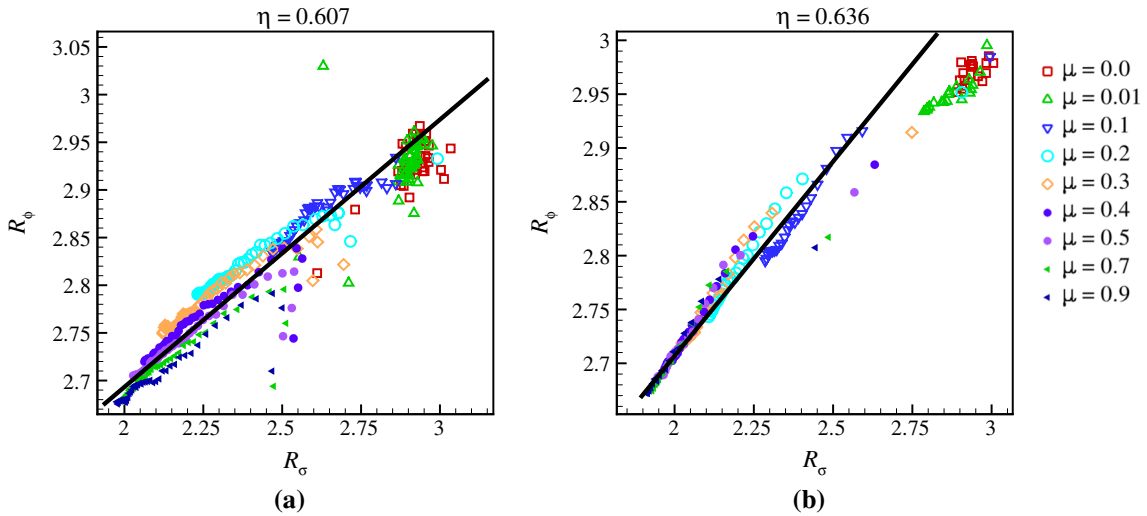

Fig. 17 R_ϕ Vs R_σ for an initial packing fraction of **a** 0.607 and **b** 0.636 with different coefficient of friction during the uniaxial compression of periodic granular assemblies

coefficient of friction. The nature of both parameters are similar with change in the coefficient of friction. Hence, these non-dimensional quantities can be correlated to each other for the uniaxial compression of mono-size periodic granular assemblies with different initial packing fraction (η) and coefficient of friction (μ). The relationship between these quantities can be plotted for different initial packing fractions in the range $0.594 \leq \eta \leq 0.64$ for a range of friction coefficients ($0.1 \leq \mu \leq 0.9$). Figure 17 shows that all the simulation data corresponding to R_ϕ and R_σ collapse on a line except for a lower ($\mu < 0.1$) coefficient of friction at higher initial packing fraction. However, coefficient of friction of most of the materials fall under the range $0.1 \leq \mu \leq 0.9$ and hence the effect of friction on the relationship between quantities R_σ and R_ϕ can be considered negligible. For a given initial packing fraction, the relation between R_ϕ and R_σ can be assumed to be a linear fit[5] with the value of coefficient of determination (R^2) being more than 0.96 for all cases. The linear relation can be expressed as,

$$R_\phi = c_1 R_\sigma + c_2, \tag{25}$$

The slope of the line is observed to be dependent on the initial packing fraction. Parameters R_ϕ and R_σ are a form of manifestation of fabric and stress, respectively. It has been reported in the past [13] that the evolution of stress is

[5] It may be noted that the linear fit is obtained from the simulation data, as shown in Fig. 17. Hence, the omission of tangential components from stress tensor equation does not affect the results in Fig. 17 and Eq. 25.

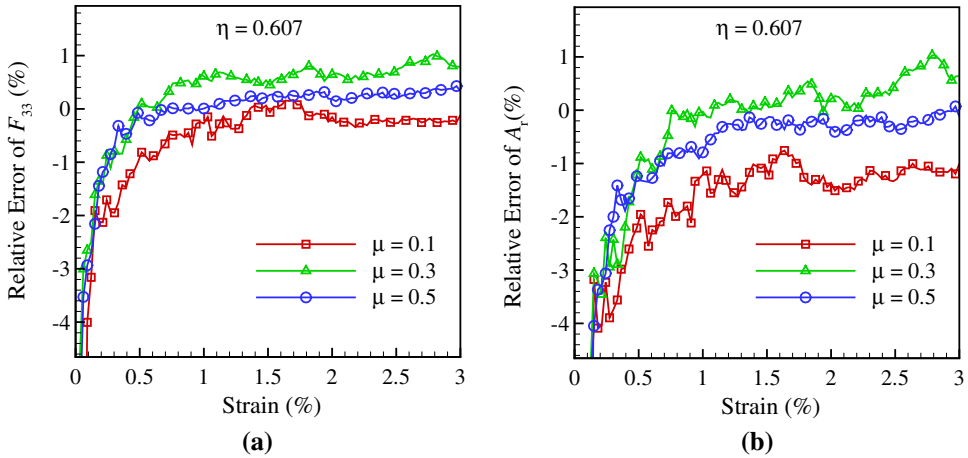

Fig. 18 Relative error of the predicted values of (**a**) F_{33} (**b**) contact anisotropy (A_r) for uniaxial compression of a monosize periodic granular assembly with η of 0.607

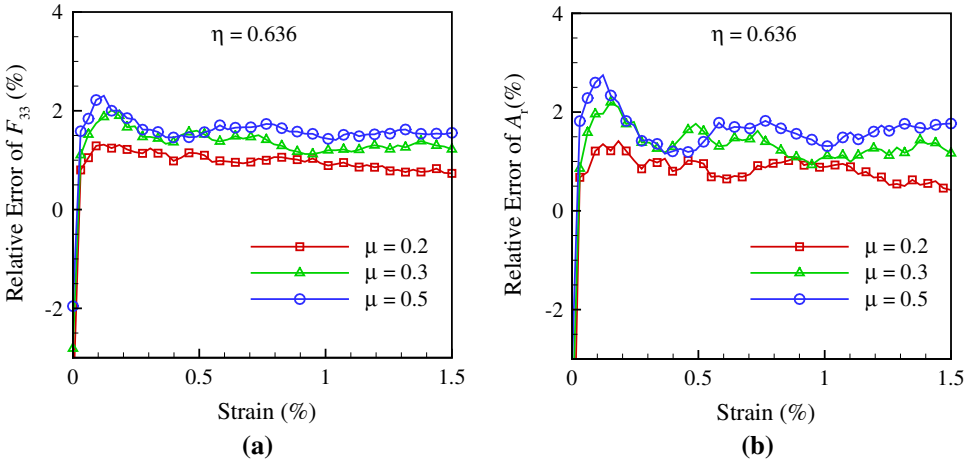

Fig. 19 Relative error of the predicted values of (**a**) F_{33} (**b**) contact anisotropy (A_r) for uniaxial compression of a monosize periodic granular assembly with η of 0.636

dependent on the initial packing fraction. Hence, the coefficients (c_1 and c_2) can be fitted as a function of initial packing fraction (η) given by

$$c_1 = 4.0311\eta - 2.1779 \text{ and } c_2 = -8.99\eta + 7.647 \tag{26}$$

It may also be noted that the variables R_ϕ and R_σ are the function of the applied strain (or instantaneous packing fraction) while c_1 and c_2 are function of initial packing fraction only. Using the assumptions from Sect. 5.3, contact anisotropy A_r can be expressed as,

$$\begin{aligned} A_r &= \frac{F_3}{F_1} = \frac{F_{33}}{F_{11}} = \frac{F_{33}}{\frac{1}{2}(F_{11}+F_{22})} = 2\phi_r \\ &= \frac{2\sigma_r}{(c_1+c_2-1)\sigma_r + c_1} \end{aligned} \tag{27}$$

The model was tested for mono-size assemblies with the initial packing fraction (η) ranging from 0.594 to 0.64 with a coefficient of friction ranging from 0.1 to 0.9 under uniaxial compression up-to 2% strain. For all the cases, the relative error (Figs. 18 and 19) was found to be within ± 4%.

Furthermore, based on the results discussed in Sect. 4, it can be inferred that the parameters c_1 and c_2 are independent of Young's modulus. In summary, the semi-analytical model presented in this section helps to decipher the microscopic picture of a monosize granular assembly directly from the macroscopic stresses eliminating the dependency on other microscopic parameters like contact forces, average coordination number, and coefficient of friction, which cannot be measured readily through experiments.

6 Summary and conclusions

In this work, the evolution of contact anisotropy in a spherical granular assembly under uniaxial compression is investigated. In particular, the effect of cyclic loading and the strain rate on the evolution of contact anisotropy and coordination number has been investigated. During cyclic loading, a packed granular assembly shows a minimum for the contact anisotropy. The knowledge of the point of minimum can be used to obtain a granular assembly with minimum contact

anisotropy leading to more isotropic thermal/electrical conduction. The contact anisotropy was found to decrease during cyclic loading, eventually saturating to a finite value after a few cycles. The hysteretic nature of the average coordination number versus strain during cyclic loading may be attributed to the persistent contact changes (creation and disruption) along the direction of compression.

For a granular assembly, subjected to high strain rate loading, the contact anisotropy shows a transient response (initial rise followed by a drop and then further increase) while for the quasi-static loading, the anisotropy increases continuously with the increase in strain. However, at large strains ($\geq 1.5\%$ macroscopic strain), the contact anisotropy seems to be independent of the strain rate. The effect of Young's modulus on the contact anisotropy was found to be negligible during quasi-static compression of the granular assembly. However, Young's modulus profoundly affects the contact creation due to high strain rate compression, thereby influencing the contact anisotropy. Significant influence of inertia was found in case of high strain rate compaction of particles with different Young's modulus while it was found to be negligible in case of quasi-static compression of the granular assembly. A semi-empirical model, correlating macroscopic stresses and the contact anisotropy, has been presented in this work. The model explores the idea of relating two new microscopic non-dimensional parameters (R_ϕ, R_σ), which exhibits a linear relationship. It is shown that coefficient of friction affects the evolution of parameters (R_ϕ, R_σ). However, the correlation between R_ϕ and R_σ is found to be independent of the coefficient of friction between the particles, average coordination number, contact forces, and the orientation data. The findings of this work are useful for manipulating the contact anisotropy of various granular assemblies generated through different methodologies. The ability to control the contact anisotropy of a granular assembly enables us to design systems with required macroscopic mechanical and thermal properties.

Compliance with ethical standards

Conflict of interest The authors declare that they have no conflict of interest.

References

1. Oda, Masanobu: Initial fabrics and their relations to mechanical properties of granular material. Soils Found. **12**(1), 17–36 (1972a)
2. Oda, Masanobu: The mechanism of fabric changes during compressional deformation of sand. Soils Found. **12**(2), 1–18 (1972b)
3. Oda, M., Konishi, J., Nemat-Nasser, S.: Some experimentally based fundamental results on the mechanical behaviour of granular materials. Géotechnique **30**, 479–495 (1980)
4. Oda, Masanobu, Konishi, Junichi, Nemat-Nasser, Siavouche: Experimental micromechanical evaluation of strength of granular materials: effects of particle rolling. Mech. Mater. **1**, 269–283 (1982)
5. Oda, Masanobu: Fabric tensor for discontinuous geological materials. Soils Found. **22**, 96–108 (1982)
6. Satake, M.: Fabric tensor in granular materials. In: Proceedings of IUTAM Symposium on Deformation and Failure of Granular materials, Delft, The Netherlands (1982)
7. Ken-Ichi, Kanatani: Distribution of directional data and fabric tensors. Int. J. Eng. Sci. **22**, 149–164 (1984)
8. Madadi, Mahyar, Tsoungui, Olivier, Lätzel, Marc, Luding, Stefan: On the fabric tensor of polydisperse granular materials in 2D. Int. J. Solids Struct. **41**, 2563–2580 (2004)
9. O'Sullivan, Catherine: Particulate Discrete Element Modelling: A Geomechanics Perspective. Taylor & Francis, Abingdon (2011)
10. Shertzer, R.: Fabric Tensors and Effective Properties of Granular Materials with Application to Snow. PhD thesis, Montana State University, Bozeman, Montana (2011)
11. Radjai, F., Delenne, J.Y., Azéma, E., Roux, S.: Fabric evolution and accessible geometrical states in granular materials. Granul Matter **14**, 259–264 (2012)
12. Kruyt, N.P.: Micromechanical study of fabric evolution in quasi-static deformation of granular materials. Mech. Mater. **44**, 120–129 (2012)
13. Annabattula, Ratna Kumar, Gan, Y., Kamlah, M.: Mechanics of binary and polydisperse spherical pebble assembly. Fusion Eng. Des. **87**, 853–858 (2012)
14. Imole, Olukayode I, Wojtkowski, Mateusz, Magnanimo, Vanessa, Luding, Stefan: Micro-macro correlations and anisotropy in granular assemblies under uniaxial loading and unloading. Phys. Rev. E **89**, 042210 (2014)
15. Yan, W.M.: Fabric evolution in a numerical direct shear test. Comput. Geotech. **36**(4), 597–603 (2009)
16. Guo, Ning, Zhao, Jidong: The signature of shear-induced anisotropy in granular media. Comput. Geotech. **47**, 1–15 (2013)
17. Yuan, Ran, Hai-Sui, Yu., Yang, Dun-Shun, Nian, Hu: On a fabric evolution law incorporating the effects of b-value. Comput. Geotech. **105**, 142–154 (2019)
18. Thornton, C.: Numerical simulations of deviatoric shear deformation of granular media. Géotechnique **50**, 43–53 (2000)
19. Kuhn, Matthew R: Heterogeneity and patterning in the quasi-static behavior of granular materials. Granul. Matter **4**(4), 155–166 (2003)
20. Hu, Minyun, O'Sullivan, Catherine, Jardine, Richard R, Jiang, Mingjing: Stress-induced anisotropy in sand under cyclic loading. Granul. Matter **12**(5), 469–476 (2010)
21. Zhao, Jidong, Guo, Ning: Unique critical state characteristics in granular media considering fabric anisotropy. Géotechnique **63**(8), 695 (2013)
22. Gao, Zhiwei, Zhao, Jidong, Li, Xiang-Song, Dafalias, Yannis F: A critical state sand plasticity model accounting for fabric evolution. Int. J. Numer. Anal. Methods Geomech. **38**(4), 370–390 (2014)
23. Gao, Zhiwei, Zhao, Jidong: Constitutive modeling of anisotropic sand behavior in monotonic and cyclic loading. J. Eng. Mech. **141**(8), 04015017 (2015)
24. Göncü, Fatih, Durán, Orencio, Luding, Stefan: Constitutive relations for the isotropic deformation of frictionless packings of polydisperse spheres. C. R. Méc. **338**(10–11), 570–586 (2010)
25. Das, Soukat Kumar, Das, Arghya: Influence of quasi-static loading rates on crushable granular materials: a dem analysis. Powder Technol. **344**, 393–403 (2019)
26. Nemat-Nasser, S., Mehrabadi, M.: Stress and fabric in granular masses. In: Jenkins JT, Satake M (eds) Studies in Applied Mechanics, vol 7, pp. 1–8. Elsevier (1983)

27. Tobita, Yoshio: Fabric tensors in constitutive equations for granular materials. Soils Found. **29**(4), 91–104 (1989)
28. Bathurst, Richard J, Rothenburg, Leo: Observations on stress-force-fabric relationships in idealized granular materials. Mech. Mater. **9**(1), 65–80 (1990)
29. Chang, Ching S, Liu, Yang: Stress and fabric in granular material. Theor. Appl. Mech. Lett. **3**(2), 021002 (2013)
30. Jodrey, W.S., Tory, E.M.: Computer simulation of close random packing of equal spheres. Phys. Rev. A **32**(4), 2347 (1985)
31. Cundall, Peter A, Strack, Otto DL: A discrete numerical model for granular assemblies. Géotechnique **29**(1), 47–65 (1979)
32. Kloss, C., Goniva, Christoph, Hager, Alice, Amberger, Stefan, Pirker, Stefan: Models, algorithms and validation for opensource DEM and CFD-DEM. Prog. Comput. Fluid Dyn. **12**, 140–152 (2012)
33. Di Renzo, Alberto, Maio, Francesco Paolo Di: An improved integral non-linear model for the contact of particles in distinct element simulations. Chem. Eng. Sci. **60**(5), 1303–1312 (2005)
34. O'Sullivan, Catherine, Cui, Liang: Micromechanics of granular material response during load reversals: combined dem and experimental study. Powder Technol. **193**(3), 289–302 (2009)
35. Soroush, Abbas, Ferdowsi, Behrooz: Three dimensional discrete element modeling of granular media under cyclic constant volume loading: a micromechanical perspective. Powder Technol. **212**(1), 1–16 (2011)
36. Sun, Jin, Sundaresan, Sankaran: A constitutive model with microstructure evolution for flow of rate-independent granular materials. J. Fluid Mech. **682**, 590–616 (2011)
37. MiDi, G.D.R.: On dense granular flows. Eur. Phys. J. E **14**(4), 341–365 (2004)
38. Johnson, K.L.: Contact Mechanics. Cambridge University Press, Cambridge (1985)
39. Gan, Yixiang, Kamlah, Marc: Discrete element modelling of pebble beds: with application to uniaxial compression tests of ceramic breeder pebble beds. J. Mech. Phys. Solids **58**(2), 129–144 (2010)
40. Bardet, J.P.: Observations on the effects of particle rotations on the failure of idealized granular materials. Mech. Mater. **18**, 159–182 (1994)